THE JOURNAL OF PHYSICAL CHEMISTRY B LETTERS

2005, *109,* 7605−7609
Published on Web 04/06/2005

Noncovalent Functionalization of Single-Walled Carbon Nanotubes with Water-Soluble Porphyrins

Jinyu Chen and C. Patrick Collier*

Division of Chemistry and Chemical Engineering, California Institute of Technology, Pasadena, California 91125

Received: January 21, 2005; In Final Form: March 11, 2005

We have employed water-soluble porphyrin molecules [*meso*-(tetrakis-4-sulfonatophenyl) porphine dihydrochloride] to solubilize single-walled carbon nanotubes (SWNTs), resulting in aqueous solutions that are stable for several weeks. The porphyrin-nanotube complexes have been characterized with absorption and fluorescence spectroscopy and with AFM. We find that the porphyrin/SWNT interaction is selective for the free base form, and that this interaction stabilizes the free base against protonation to the diacid. Under mildly acidic conditions nanotube-mediated *J*-aggregates form, which are unstable in solution and result in precipitation of the nanotubes over the course of a few days. Porphyrin-coated SWNTs can be precisely aligned on hydrophilic poly(dimethylsiloxane) (PDMS) surfaces by combing SWNT solution along a desired direction and then transferred to silicon substrates by stamping. Parallel SWNT patterns have been fabricated in this manner.

Introduction

The unique structural, mechanical and electronic properties of single walled carbon nanotubes (SWNTs) have made these promising materials for device fabrication.[1−14] To effectively utilize SWNTs as building blocks for nanotechnology, nanotubes have been covalently and noncovalently functionalized in a number of ways to render them soluble in aqueous or organic solutions[15−21] and to gain precise control over nanotube orientation and location. There are two general strategies for gaining spatial control of SWNTs. In the direct-growth strategy, nanotube length, location, and orientation can be controlled using pre-patterned catalyst and chemical vapor deposition (CVD).[3,13,14,22−25] In the post-growth strategy, nanotubes can be aligned by various methods, including biomolecular recognition,[4,26] manipulation by an atomic force microscope (AFM) tip,[5] application of an electric field[27] or a magnetic field,[28] deposition on chemically patterned surfaces,[29] alignment by gas-flow,[30] or dip-coating washing.[31] For many applications it is important that the inherent functionality of the carbon nanotubes not be altered or destroyed by high-temperature CVD, covalent chemical functionalization steps or various applied fields.

It has been reported that zinc protoporphyrin IX (ZnPP) noncovalently binds to SWNTs and renders them soluble in DMF or DMSO solution.[32] More recently, it has been discovered that a *meso*-hexadecyloxyphenyl-substituted porphyrin is selective in noncovalently solubilizing semiconducting single-walled carbon nanotubes in organic solvents.[33] Functionalization of SWNTs with porphyrins could supply the nanotubes with many of the porphyrin's unique intrinsic properties, such as (electro) luminescence, photovoltaic properties, and biocompatibility.

We report here a facile approach to noncovalently functionalize SWNTs in aqueous solution with a water-soluble ionic porphyrin, *meso*-(tetrakis-4-sulfonatophenyl) porphine (H_2TPPS^{4-}). Porphyrin/SWNT solutions in water have been prepared that are stable for weeks, without covalent chemical functionalization of the tubes or the use of surfactants. We have characterized the porphyrin/SWNT solutions with UV−visible absorption and fluorescence spectroscopic measurements as functions of pH, which show that the free base form of the porphyrin selectively interacts with the nanotubes and is mainly responsible for solubilizing them in water. The interaction with the SWNTs inhibits the protonation of the free base to the diacid. Under mildly acidic conditions, *J*-aggregates form on the nanotubes. We found that the fluorescent properties of the free base and diacid forms of H_2TPPS^{4-} were not significantly perturbed by the nanotubes, but that emission from the *J*-aggregates was completely quenched. Finally, the solubilization procedure has allowed us to align SWNTs, by combing the nanotubes from aqueous solution on clean poly(dimethylsiloxane) (PDMS) stamps, followed by transfer printing of the tubes from PDMS to silicon or glass surfaces.

Experimental Section

The porphyrin *meso*-(tetrakis-4-sulfonatophenyl) porphine (H_4TPPS^{2-}) was purchased from Frontier Scientific as the dihydrochloride salt of the diacid (**1**, Figure 1A). SWNTs (HiPco, Carbon Nanotechnologies) were used as received without further purification. Millipore water (18 MΩ) was used throughout. HCl (aq) was from J. T. Baker and NH_4OH (aq) was from E. M. D. Chemicals. UV−visible absorption spectroscopy was carried out with a Uvikon 933 spectrophotometer, and fluorescence measurements were performed on a ISS K2 fluorometer. Tapping mode AFM imaging was performed with a MultiMode with Nanoscope IV controller from Digital Instruments. The silicon substrates used for AFM imaging had been previously cleaned with "piranha" solution (3:7 (v/v)

* Corresponding author. E-mail: collier@caltech.edu.

10.1021/jp050389i CCC: $30.25

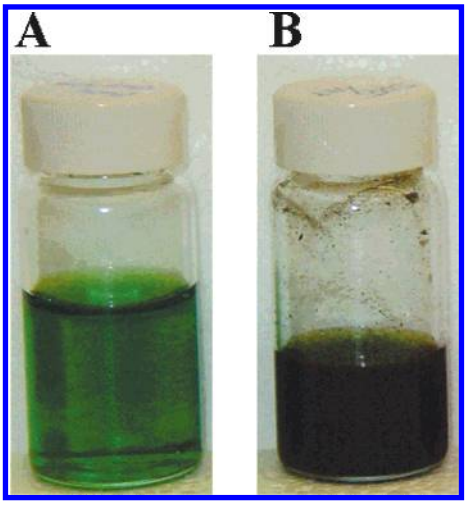

Figure 1. Aqueous solutions of (a) **1** (0.6 mg/mL) and (b) SWNT-**1** complex.

SCHEME 1: *meso*-(Tetrakis-4-sulfonatophenyl) Porphine (H_4TPPS^{2-})

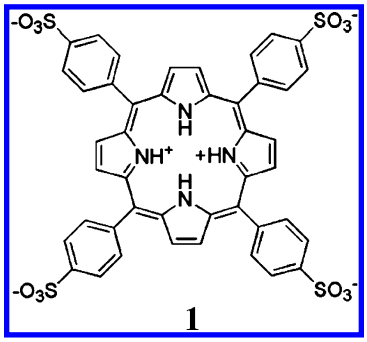

mixture of 30% H_2O_2 and H_2SO_4; CAUTION: this mixture reacts violently with organic materials).

Results and Discussion

The addition of the H_4TPPS^{2-} salt to pure water results in an equilibrium between the diacid and free base forms of the porphyrin ($pKa_1 = 4.86$, $pKa_2 = 4.96$), which is pH dependent. Both forms have a characteristic intense absorption band near 400 nm called the Soret band and a series of less intense absorption features at longer wavelengths called Q-bands (all due to $\pi-\pi^*$ electronic transitions), which can be used to quantify their relative concentrations. Under strongly acidic conditions (pH <1) or in the presence of various cationic species, *J*-aggregates of H_4TPPS^{2-} can form, which exhibit an intense narrow absorption band at 490 nm.[34]

A freshly prepared solution of H_4TPPS^{2-} salt dissolved in pure water (0.6 mg/mL, 25 mL) results in a deep green-colored transparent solution with pH = 4.66, Figure 1A. After addition of SWNTs (0.1 mg), the porphyrin solutions were ultrasonicated for thirty minutes to 1 h (ULTRASonik 57×) and left standing for two to 3 days, resulting in a black-colored solution (Figure 1B). 100 μL of the supernatant of this solution was carefully removed by pipet and diluted to 6 mL. The UV−vis absorption spectrum from 460 to 750 nm of this solution is shown as the solid line in Figure 2A. Survey spectra covering the 200−900 nm wavelength range are included in the Supporting Information, which show the positions of the Soret absorption band of the free base at 413 nm and the peaks belonging to the diacid at 435 and 646 nm. The positions of these bands were not perturbed by interactions with the nanotubes, as seen by comparison to the spectrum from an aqueous solution containing the same concentration of porphyrin (at the same pH) but with no SWNTs (dashed line). The new peaks at 492 and 712 nm in the presence of the SWNTs are from *J*-aggregates that have nucleated on the nanotubes. These peaks are clearly absent in the porphyrin solution not containing SWNTs (dashed line in Figure 2A, which was the same with or without sonication). Their absence can be correlated with the lack of features in the 700−900 nm wavelength range (dashed line in Figure 2B), while the solution containing SWNTs has broad adsorption throughout this range, due to the characteristic interband transitions of the nanotubes.[35]

The *J*-aggregate/SWNT complexes were not stable in solution. After about 1 day, both the absorption peak at 490 nm and the broad absorption from 750 to 900 nm dropped to about 1/4 of their original intensity. These spectral changes were correlated with the appearance of black flocs that precipitated out of solution. The loss of the *J*-aggregate absorption did not correspond to a transition from the aggregate state to free base or diacid in solution since the peaks corresponding to the free base and diacid absorption did not change significantly.

The precipitates were collected on a cellulose acetate membrane (0.22 μm pore size, Corning) using vacuum filtration. The membrane was washed continuously with pure water until the washes became colorless and then dried in a desiccator at room temperature for 2 days. The membrane was cut into strips, re-immersed in pure water, and subjected to ultrasonication for 2 h, resulting in a grayish supernatant with some residual dark green material left on the membrane strips and walls of the glass vial. The UV−vis absorption spectrum of this redispersed solution (pH = 6.66) showed the presence of SWNTs coexisting only with free base porphyrins, with no diacid or *J*-aggregates. The absorption spectrum of the filtrate (pH = 4.38) on the other hand consisted of peaks from the free base and diacid, but without SWNTs or *J*-aggregates. This evidence indicates that it is the free base form of H_4TPPS^{2-} that selectively binds to SWNTs and renders them soluble in aqueous solution, and not the diacid or other forms, in accordance with a previous report describing porphyrin solubilization of SWNTs in nonaqueous solvents.[33] This conclusion is further supported by adjusting the pH of a fresh porphyrin solution with NH_4OH (aq) before mixing with SWNTs to quantitatively drive the acid/base equilibrium toward the free base; the absorption spectrum of this solution (pH = 7.1) showed the presence of only free base porphyrin and SWNTs.

Tapping mode AFM images of drop-cast films onto clean silicon surfaces from the original "as-prepared" porphyrin-SWNT solution showed a large background from porphyrin aggregates adsorbed on the substrate surface, as well as porphyrin-nanotube complexes. Included in the Supporting Information is a representative AFM image of an isolated SWNT or small nanotube bundle decorated with what we interpret to be porphyrin aggregates. Samples prepared from the redispersed solution showed substantially less porphyrin aggregate background compared to the original as-prepared solution, allowing us to obtain a histogram of the functionalized nanotube diameter distribution from 129 AFM height images, which is included in the Supporting Information. The largest components to the distribution consisted of 0.5 to 1.0 nm features, which was consistent with the diameters of individual nanotubes produced by the HiPco process,[36] although the tail of the distribution of diameters extended out to 7 nm. Because of the nucleation of porphyrin aggregates on the nanotubes, we could not ascertain whether the larger diameter images were due to small SWNT

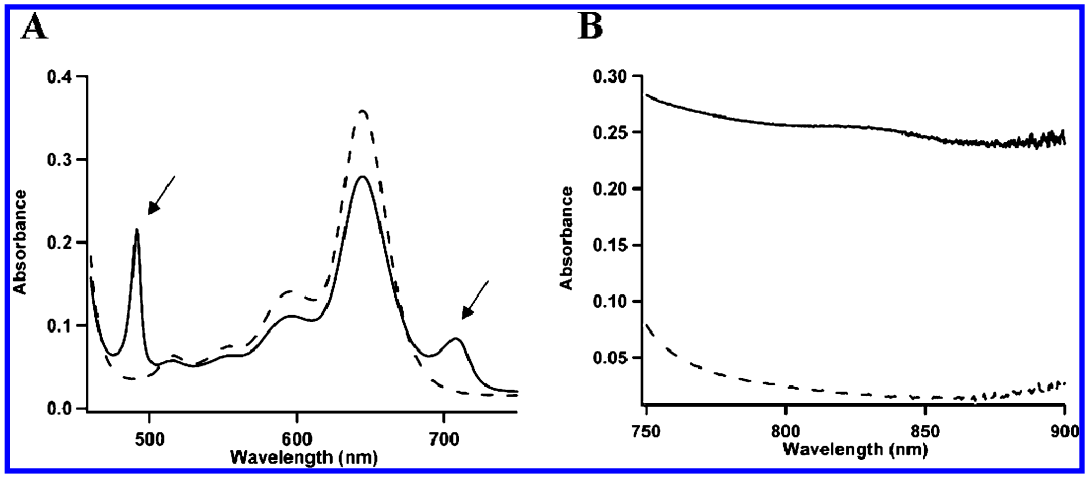

Figure 2. Absorption spectra of porphyrin/SWNT aqueous solutions (solid lines) and pure porphyin solutions containing no SWNTs (dashed lines). (a) Spectra from 460 to 750 nm. Arrows indicate peaks due to *J*-aggregates observed only in the porphyrin/SWNT solution. (b) Spectra from 750 to 900 nm indicating the presence (solid line) or absence (dashed line) of soluble SWNTs. The porphyrin/SWNT solution concentrations used in (b) were 15 times greater than in (a).

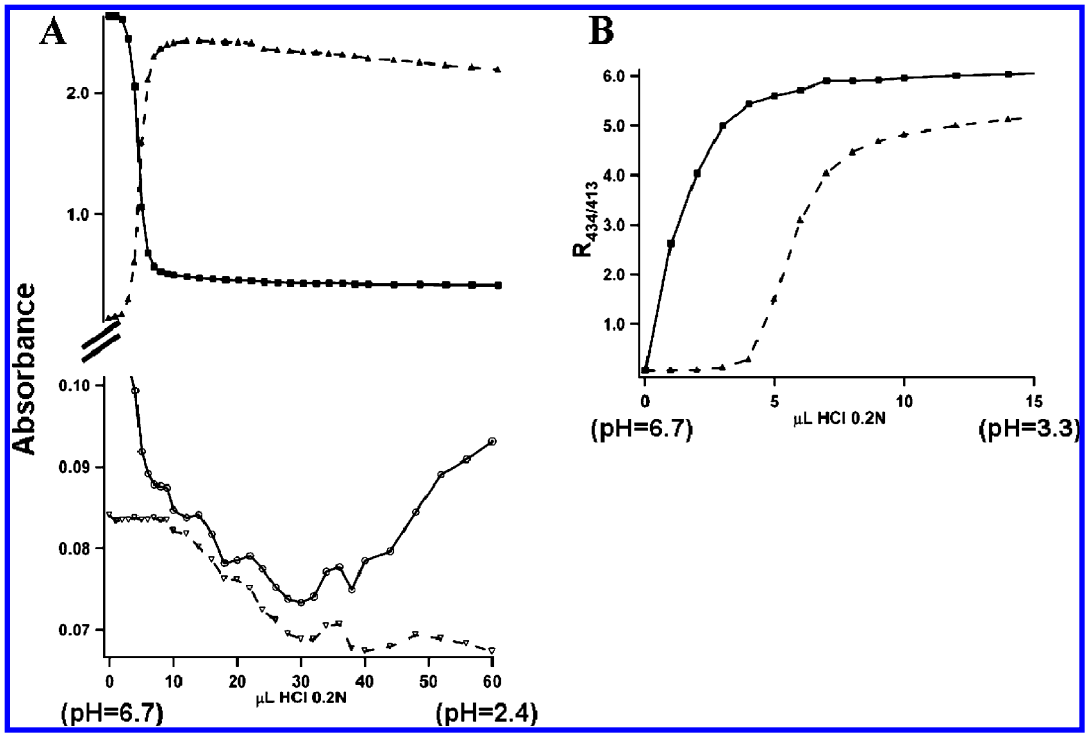

Figure 3. (a) Trends in the optical absorbance maxima of the porphyrin free base at 413 nm (filled squares), diacid at 434 nm (filled triangles), *J*-aggregates at 490 nm (open circles), and SWNTs at 740 nm (open triangles) as functions of volume of added acid (0.2N HCl). (b) Ratios of the absorbance maxima of the diacid (434 nm) to the free base (413 nm) as functions of added acid for porphyrin/SWNT solution (dashed line) and pure porphyrin solution containing no SWNTs (solid line).

bundles or were from individual nanotubes with adsorbed porphyrin aggregates.

We also tried to determine if individual porphyrin-wrapped SWNTs were present in the redispersed solution from the SWNT interband transitions in the optical absorption spectra recorded from 500 to 900 nm, in the manner described by O'Connell et al. (Supporting Information).[37] While the SWNT interband absorption features in the 700−900 nm wavelength range were more intense and better resolved in the spectrum of the redispersed solution compared to that of the original as-prepared solution (Figure 2B), there was also substantial spectral overlap from the tails of the Q-bands of the porphyrins, which completely overwhelmed SWNT transitions to the blue of 700 nm. We were thus unable to determine from the optical spectra if we had solubilized individual SWNTs or small bundles.

We explored the pH dependence of the porphyrin/SWNT interactions in more detail by monitoring the absorption spectra of the redispersed solution as functions of titration with 0.2 N HCl(aq). The trends in the optical signatures of the porphyrin free base, diacid, *J*-aggregates, and SWNTs are plotted relative to each other in Figure 3A. The actual absorption spectra from the titrations that generated these trends are included in the Supporting Information.

Before addition of HCl (initial pH = 6.66, initial volume = 6 mL), only the porphyrin free base and SWNT optical signatures were seen. Titration with 10 μL of acid was enough to quantitatively convert the free base form (monitored at 413 nm) to the diacid (434 nm). However, the onset of the diacid absorption was significantly delayed relative to that of an identically prepared control solution (same initial pH) lacking

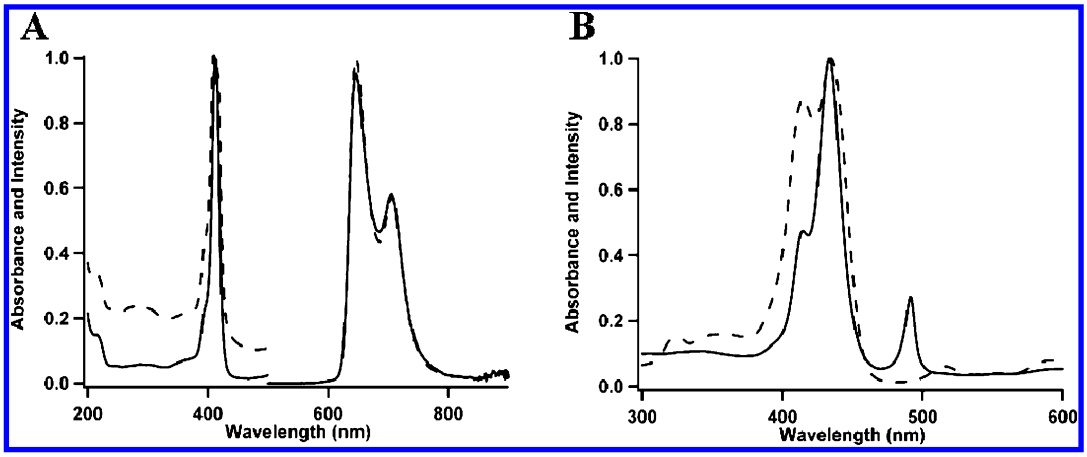

Figure 4. (a) Normalized absorption and fluorescence emission spectra of porphyrin/SWNT solution (dashed line) and solution containing only porphyrin (solid line). (b) Normalized absorption (solid line) and excitation (dashed line) spectra taken from the same porphyrin/SWNT solution. The excitation spectrum was monitored at 700 nm.

SWNTs. This can be seen by plotting the ratio of the diacid absorbance over that of the free base as a function of added HCl, Figure 3B. Due to interactions of the free base with the SWNTs, more HCl (aq) was required to protonate the porphyrin to the diacid form compared to the pure porphyrin solution lacking nanotubes. We believe there are two reasons for this difference. First, the association of the free base with the nanotubes decreases the accessibility of the unprotonated nitrogen atoms in the porphyrin core for attack by hydronium ions. Second, it is known that the average equilibrium structure of the H_2TPPS^{4-} porphyrin molecule in the free base state is planar while the pyrrole rings in the diacid form are tilted significantly away from planarity.[38] It is plausible that interactions with the π-network of the SWNT sidewalls stabilize the planar free base form.[39] This reasoning is also consistent with our finding that the free base form specifically associates with and solubilizes the SWNTs in water. As the diacid optical signature grows in intensity and the free base absorption decreases, the absorption due to the solubilized SWNTs also decreases.

Additional HCl aliquots result in the formation of *J*-aggregates, monitored at 490 nm. The decrease in the absorption at 490 nm between 10 and 30 μL added HCl is not associated with the optical signature from *J*-aggregates but is due to the decrease of the high-frequency edge of the Q-band of the free base. As the *J*-aggregate signal grows in intensity from 30 to 60 μL added HCl, the diacid absorption decreases and the SWNT absorption stays roughly constant, consistent with a picture involving aggregation of diacid monomers onto nanotubes at low pH. The absorption signals from the *J*-aggregate/SWNT complexes dropped somewhat after this solution was left standing for 12 h due to precipitation (final pH = 2.4), but not to the extent of the original dispersion made without adding excess acid or base (pH = 4.66), which suggests that the solubility of these nanocomposites may be pH dependent.

Fluorescence spectra were acquired from an as-prepared porphyrin-SWNT solution, the redispersed solution and a control solution containing porphyrins but no SWNTs. All three solutions exhibited strong fluorescence in the 625−750 nm wavelength region when excited at 413 nm corresponding to emission from the free base and the diacid, but no fluorescence was observed from *J*-aggregates. Figure 4A shows absorption and fluorescence emission spectra of the porphyrin/SWNT redispersed complex and a solution of pure porphyrin, normalized for concentration (7.8 μM, based on the extinction coefficient of the Soret band, $\epsilon_{413} = 500\,000\ M^{-1}\ cm^{-1}$)[40] and prepared at identical pH (6.9). The normalized fluorescence profile of the porphyrin/SWNT redispersed solution was approximately the same as that of pure porphyrin, indicating that the interactions with the nanotubes did not significantly quench or otherwise perturb the emission from the free base or the diacid.

Figure 4B shows absorption and fluorescence excitation spectra taken within minutes of each other from a fresh "as-prepared" porphyrin-SWNT solution (pH = 4.66). The excitation spectrum was monitored at 700 nm, which is near the emission maximum for *J*-aggregates of H_4TPPS^{2-}.[41] The intense peak at 490 nm from the *J*-aggregates is evident in the absorption spectrum, but is completely absent in the excitation spectrum. Apparently, efficient energy transfer to the nanotubes completely quenches fluorescence from the *J*-aggregates. This suggests that the aggregates are in more intimate contact with the nanotube sidewalls, presumably through strong $\pi-\pi$ interactions. One reason this quenching is not seen for the free base and diacid is that these forms, and in particular the free base, associate with the SWNTs more through long-range electrostatic interactions, and are not as tightly bound to the nanotubes as the *J*-aggregates.

The trends in the optical absorption and fluorescence spectra as functions of pH provide clues as to the nature of the interactions of the various forms of the porphyrin with carbon nanotubes. The free base of the porphyrin (H_2TPPS^{4-}) has the combination of planarity of the porphyrin ring and the highest negative charge density from the anionic sulfonate groups, which makes it the most effective form at dispersing and stabilizing SWNTs in solution, consistent with a recent report that the negatively charged phosphate backbone of DNA helps disperse SWNTs in water.[42] The diacid form (H_4TPPS^{2-}) is nonplanar and has less negative charge, and stabilizes SWNTs in water to a lesser extent, as seen by the decreased optical absorption from the nanotubes at lower pH in Figure 3A. Finally, *J*-aggregates, once nucleated, can form insoluble precipitates by diffusion-limited aggregation with an average size on the order of hundreds of nm.[34]

The ability to disperse porphyrin-functionalized SWNTs in aqueous solution allowed us to align the nanotubes on PDMS stamps via a combing procedure followed by transfer of the aligned tubes onto silicon or glass substrates for potential device fabrication. One drop (50 μL) of the H_4TPPs^{2-}/SWNT aqueous solution was pipetted onto the surface of a clean PDMS stamp that had been pretreated in an oxygen plasma cleaner (Harrick) prior to use. A glass coverslip was placed at the far edge of the drop and slid over the surface as shown in Figure 5A. The drag

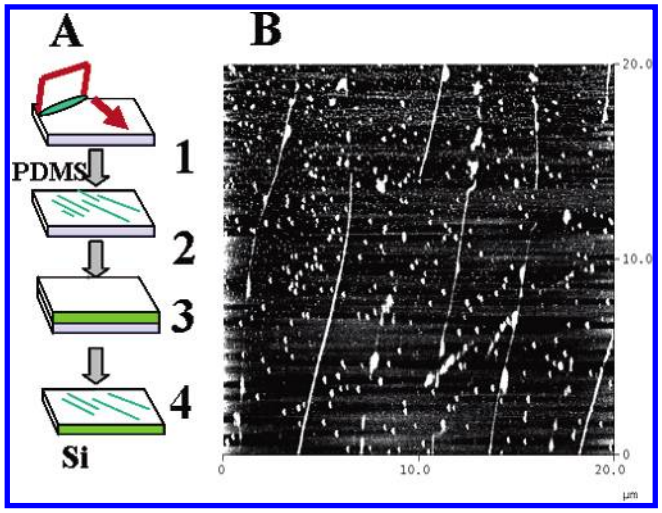

Figure 5. (a) Alignment of porphyrin functionalized SWNTs onto PDMS stamps by combing followed by transfer printing of the aligned nanotubes onto a silicon substrate, (b) imaged with tapping mode AFM.

forces acting at the surface of the stamp aligned the nanotubes along the sliding direction. After the PDMS surface had been allowed to dry in air, it was contacted to a clean silicon wafer for 1 h. With this step, the pre-aligned porphyrin-functionalized SWNTs were transferred to the silicon wafer. Figure 5B is a representative 20 μm × 20 μm height image of several aligned SWNTs on silicon captured with tapping mode AFM.

Although there is a large background from adsorbed porphyrin aggregates on the silicon substrate in Figure 5B, one can still see multiple SWNTs (or small bundles of SWNTs) aligned parallel to one other over distances on the order of 20 μm. Apparently, the combing and transferring procedure results in the preferential alignment of the longest SWNTs, which has important implications for large scale fabrication of functionalized SWNT arrays. Generally, we found that this degree of SWNT alignment extended over the entire surface of the silicon wafer that had been in contact with the PDMS stamp.

Conclusion

Absorption and fluorescence measurements of aqueous solutions of the water-soluble porphyrin H_2TPPs^{4-} complexes with SWNTs indicate that the free base form is primarily responsible for rendering the nanotubes soluble in water, while the stabilizing interactions with the tubes makes it more difficult to protonate the porphyrin to the diacid form. *J*-aggregates nucleate on the nanotubes under mildly acidic conditions (pH∼5). Efficient energy transfer between the *J*-aggregates and the nanotubes results in complete quenching of fluorescence while emission from the free base and the diacid remains largely unaffected. Water soluble porphyrin/SWNTs can be aligned on PDMS stamps and transfer printed onto silicon substrates, which may be useful for future device fabrication.

Acknowledgment. This work was supported by Arrowhead Research. We thank Yoshie Narui for help with the fluorescence measurements.

Supporting Information Available: Absorption spectra of porphyrin/SWNT complexes, tapping mode AFM image of porphyrin-functionalized SWNT and histogram of porphyrin-SWNT diameter distribution from AFM images. This material is available free of charge via the Internet at http://pubs.acs.org.

References and Notes

(1) Baughman, R. H.; Zakhidov, A. A.; de Heer, W. A. *Science* **2002**, *297*, 787.
(2) Tans, S. J.; Verschueren, A. R. M.; Dekker, C. *Nature* **1998**, *393*, 49.
(3) Li, S.; Yu, Z.; Yen, S.-F.; Tang, W. C.; Burke, P. J. *Nano Lett.* **2004**, *4*, 753.
(4) Keren, K.; Berman, R. S.; Buchstab, E.; Sivan, U.; Braun, E. *Science* **2003**, *302*, 1380.
(5) Postma, H. W. Ch.; Teepen, T.; Yao, Z.; Grifoni, M.; Dekker, C. *Science* **2001**, *293*, 76.
(6) Derycke, V.; Martel, R.; Appenzeller, J.; Avouris, Ph. *Nano Lett.* **2001**, *1*, 453.
(7) Rinzler, A.; Hafner, J. H.; Nikolaev, P.; Lou, L.; Kim, S. G.; Tomanek, D.; Nordlander, P.; Colbert, D. T.; Smalley, R. E. *Science* **1995**, *269*, 1550.
(8) Dai, H.; Hafner, J. H.; Rinzler, A. G.; Colbert, D. T.; Smalley, R. E. *Nature* **1996**, *384*, 147.
(9) Wong, S. S.; Joselevich, E.; Woolley, A. T.; Cheung, C. L.; Lieber, C. M. *Nature* **1998**, *394*, 52.
(10) Kong, J.; Franklin, M. R.; Zhou, C.; Chapline, M. G.; Peng, S.; Cho, K.; Dai, H. *Science* **2000**, *287*, 622.
(11) Collins, P. G.; Bradley, K.; Ishigami, M.; Zettl, A. *Science* **2000**, *287*, 1801.
(12) Tombler, T. W.; Zhou, C.; Alexseyev, L.; Kong, J.; Dai, H.; Liu, L.; Jayanthi, C. S.; Tang, M.; Wu, S. Y. *Nature* **2000**, *405*, 769.
(13) Qi, P.; Vermesh, O.; Grecu, M.; Javey, A.; Wang, Q.; Dai, H.; Peng, S.; Cho, K. J. *Nano Lett.* **2003**, *3*, 347.
(14) Lin, Y.; Lu, F.; Tu, Y.; Ren, Z. *Nano Lett.* **2004**, *4*, 191.
(15) Krstic, V.; Duesberg, G. S.; Muster, J.; Burghard M.; Roth, S. *Chem. Mater.* **1998**, *10*, 2338.
(16) Nakashima, N.; Kobae, N. H.; Sagara T.; Murakami, H. *Chem. Phys. Chem.* **2002**, *3*, 456.
(17) O'Connell, M. J.; Boul, P.; Ericson, L. M.; Huffman, C.; Wang, Y.; Haroz, E.; Kuper, C.; Tour, J.; Ausman, K. D.; Smalley, R. E. *Chem. Phys. Lett.* **2001**, *342*, 265.
(18) Star, A.; Stoddart, J. F.; Steuerman, D.; Diehl, M.; Boukai, A.; Wong, E. W.; Yang, X.; Chung, S.-W.; Choi H.; Heath, J. R. *Angew. Chem., Int. Ed.* **2001**, *40*, 1721.
(19) Chen, J.; Liu, H.; Weimer, W. A.; Halls, M. D.; Waldeck D. H.; Walker, G. C. *J. Am. Chem. Soc.* **2002**, *124*, 9034.
(20) Steuerman, D. W.; Star, A.; Narizzano, R.; Choi, H.; Ries, R. S.; Nicolini, C.; Stoddart J. F.; Heath, J. R. *J. Phys. Chem. B* **2002**, *106*, 3124.
(21) Nakashima, N.; Tomonari Y.; Murakami, H. *Chem. Lett.* **2002**, 638.
(22) Huang, L.; Wind, S. J.; O'Brien, S. P. *Nano Lett.* **2003**, *3*, 299.
(23) Zhang, Y.; Chang, A.; Cao, J.; Wang, Q.; Kim, W.; Li, Y.; Morris, N.; Yenilmez, E.; Kong, J.; Dai, H. *Appl. Phys. Lett.* **2001**, *79*, 3155.
(24) Huang, S.; Cai, X.; Liu, J. *J. Am. Chem. Soc.* **2003**, *125*, 5636.
(25) Joselevich, E.; Lieber, C. M. *Nano Lett.* **2002**, *2*, 1137.
(26) Xin, H.; Woolley, A. T. *J. Am. Chem. Soc.* **2003**, *125*, 8710.
(27) Nagahara, L. A.; Amlani, I.; Lewenstein, J.; Tsui, R. K. *Appl. Phys. Lett.* **2002**, *80*, 3826.
(28) Walters, D. A.; Casavant, M. J.; Qin, X. C.; Huffman, C. B.; Boul, P. J.; Ericson, L. M.; Haroz, E. H.; O'Connell, M. J.; Smith, K.; Colbert, D. T.; Smalley, R. E. *Chem. Phys. Lett.* **2001**, *338*, 14.
(29) Choi, K. H.; Bourgoin, J. P.; Auvray, S.; Esteve, D.; Duesberg, G. S.; Roth, S.; Burghard, M. *Surf. Sci.* **2000**, *462*, 195.
(30) Xin, H.; Woolley, A. T. *Nano Lett.* **2004**, *4*, 1481.
(31) Ko, H.; Peleshanko, S.; Tsukruk, V. V. *J. Phys. Chem. B* **2004**, *108*, 4385.
(32) Murakami, H.; Nomura T.; Nakashima, N. *Chem. Phys. Lett.* **2003**, *378*, 481.
(33) Li, H.; Zhou, B. Lin, Y.; Gu, L.; Wang, W.; Fernando, K. A. S.; Kumar, S.; Allard, L. F.; Sun, Y.-P. *J. Am. Chem. Soc.* **2004**, *126*, 1014.
(34) Castriciano, M. A.; Romeo, A.; Villari, V.; Micali, N.; Scolaro, L. M. *J. Phys. Chem. B* **2003**, *107*, 8765.
(35) Chiang, I. W.; Brinson, B. E.; Huang, A. Y.; Wills, P. A.; Bronikowski, M. J.; Margrave, J. L.; Smalley, R. E.; Hauge, R. H. *J. Phys. Chem. B* **2001**, *105*, 8297.
(36) Zhou, W.; Ooi, Y. H.; Russo, R.; Papanek, P.; Luzzi, D. E.; Fischer, J. E.; Bronikowski, M. J.; Willis, P. A.; Smalley, R. E. *Chem. Phys. Lett.* **2001**, *350*, 6.
(37) O'Connell, M. J.; Bachilo, S. M.; Huffman, C. B.; Moore, V. C.; Strano, M. S.; Haroz, E. H.; Rialon, K. L.; Boul, P. J.; Noon, W. H.; Kittrell, C.; Ma, J.; Hauge, R. H.; Weisman, R. B.; Smalley, R. E. *Science* **2002**, *297*, 593.
(38) Stone, A.; Fleischer, E. B. *J. Am. Chem. Soc.* **1968**, *90*, 2735.
(39) Hunter, C. A.; Sanders, J. K. *J. Am. Chem. Soc.* **1990**, *112*, 5525.
(40) Koti, A. S. R.; Perisamy, N. *J. Mater. Chem.* **2002**, *12*, 2312.
(41) Ohno, O.; Kaizu, Y.; Kobayashi, H. *J. Chem. Phys.* **1993**, *99*, 4128.
(42) Zheng, M.; Jagota, A.; Semke, E. D.; Diner, B. A.; McLean, R. S.; Lustig, S. R.; Richardson, R. E.; Tassi, N. G. *Nature Mater.* **2003**, *2*, 338.